The Influence of Surface Characteristics, Topography, and Continentality on Mountain Permafrost in British Columbia

A. Hasler[1, 2], M. Geertsema[1], V. Foord[1], S. Gruber[3], and J. Noetzli[4]

[1] Ministry of Forest, Land and Natural Resources Operation of British Columbia, 1044 Fifth Avenue, Prince George BC V2L 5G4, Canada.

[2] Department of Geosciences, University of Fribourg, Chemin du Musee 4, CH-1700 Fribourg, Switzerland.

[3] Department of Geography and Environmental Studies, Carleton University, 1125 Colonel By Drive, Ottawa ON K1S 5B6, Canada

[4] Glaciology, Geomorphodynamics and Geochronology, Department of Geography, University of Zurich, Winterthurerstr 190, CH-8057 Zurich, Switzerland.

Correspondence to: Andreas Hasler, Department of Geosciences, University of Fribourg, Chemin du Musee 4, CH-1700 Fribourg, Switzerland, andreas.hasler@unifr.ch

To check the proofs: Andreas Hasler, Department of Geosciences, University of Fribourg, Chemin du Musee 4, CH-1700 Fribourg, Switzerland, andreas.hasler@unifr.ch, phone number: +41 26 300 9012, fax: +41 26 300 9746

Abstract

Thermal offset and surface offset describe mean annual ground temperature relative to mean annual air temperature, and for permafrost modelling, they are often predicted as a function of surface characteristics and topography. As macro-climatic conditions influence the effectiveness of the underlying processes, knowledge on surface- and topography-

specific offsets is not easily transferable between regions, limiting the applicability of empirical permafrost distribution models over areas with strong macro-climatic gradients.
In this paper we describe surface and thermal offsets derived from distributed measurements at seven field sites in British Columbia. Key findings are i) a surprisingly small variation of the surface offsets between different surface types; ii) small thermal offsets at all sites (excluding wetlands and peat); iii) a clear influence of the micro-topography at wind exposed sites (snow cover erosion); iv) a north-south difference of the surface offset of 4°C in vertical bedrock and of 1.5–3°C on open (no canopy) gentle slopes; v) only small macro-climatic differences possibly caused by the inverse influence of snow cover and annual air temperature amplitude. These findings suggest, that topo-climatic factors strongly influence the mountain permafrost distribution in British Columbia.

KEY WORDS: Mountain permafrost; Surface offset, Thermal offset, Continentality, British Columbia

1. Introduction

To estimate permafrost distribution and characteristics knowledge of site specific coupling between the lower atmosphere and the ground is needed. Surface offsets (SO), defined as MAGST minus MAAT (where MAGST is the mean annual ground-surface temperature and MAAT is the mean annual air temperature), and thermal offsets (TO), defined as TTOP minus MAGST (where TTOP is the mean annual temperature at the top of permafrost), are terms to describe this coupling (Lunardini, 1978). These offsets depend on local climatic and topographic conditions as well as the surface characteristics because these conditions cause a large variability in (solar and long-wave) radiation, snow cover insulation and other phenomena affecting near-surface heat transfer. Empirical permafrost models implicitly apply the concept of these offsets by estimating the ground thermal conditions (or permafrost probability) based on MAAT (or elevation) and proxy-variables of the topo-

51 climatic effects and the surface conditions (Riseborough et al., 2008). The assessment of the
52 variation and control of surface and thermal offsets in the mountain ranges of British
53 Columbia, Canada, is therefore essential for an estimation of the province-wide permafrost
54 distribution and the analysis of related natural hazards. This study presents the first
55 distributed ground temperature records in potential permafrost areas of this region, which
56 are necessary for such a task.

57 For mountain permafrost the influence of (steep) topography is well-described for some
58 mid-latitude mountain ranges considering meso-scale variability in solar radiation
59 (insolation), air temperature, snow deposition and snow redistribution (cf. Harris et al.,
60 2009 for a literature review on this subject). The influence of surface characteristics on
61 mountain permafrost is addressed in some case studies (Gubler et al., 2011; Schneider et al.,
62 2012) for high-alpine surface types. British Columbia's higher latitude with mountain
63 permafrost extending below tree line, however, alters the influence of the surface
64 characteristics and topography compared to the permafrost in the Alps or other mid-latitude
65 mountain ranges. Studies elsewhere in Canada (Harris, 2008; Bonnaventure et al., 2012) are
66 either not spatially distributed or rely on BTS measurements so they can not be easily
67 extrapolated (without local permafrost evidences) to our study region. Hence, we aim to
68 estimate the region-specific variation of the temperature offsets (SO, TO) dependent at
69 micro- and meso-scale gradients in surface characteristics and topography.

70 At the macro-climatic scale, variations in MAAT are the primary determinant of
71 permafrost occurrence (Throop et al., 2012). While MAAT variations are relatively easily
72 captured in flat terrain with interpolation products or climate re-analysis datasets, mountain
73 topography adds large uncertainties to such estimates due to variations in the air
74 temperature lapse rate (Fiddes and Gruber, 2014). Further, an important issue to estimate
75 the permafrost conditions on the large-scale is the question if the surface offset (SO) is
76 strongly influenced by macro-climatic parameters (e.g. precipitation and continentality).

These macro-climatic parameters are thought to modify the effectiveness of the physical processes responsible for the surface offsets and cause, together with variations in MAAT alone, meridional gradients on the continental scale of the lower limit of mountain permafrost (cf. King, 1986; Harris, 1989) and the southern extent of lowland permafrost (Harris, 1986). Guodong and Dramis (1992) report different dependencies of the lower limit of mountain permafrost on continentality found for different latitudes in China. A recent study on the Alpine-wide permafrost distribution found a slightly positive dependency on precipitation of the probability of rock glaciers being active (Boeckli et al., 2012). A field investigation from different sites in Norway attributed the decrease of the lower limit of mountain permafrost to the decrease in snow water equivalent with increasing continentality as well as to effects of predominant surface types (Farbrot et al., 2011). This question is another focus of this study because British Columbia and our field sites span a large gradient in macro-climatic conditions.

Due to the patchy characteristics of our data, this paper comprises a description of the data processing and resulting uncertainties in SO and TO (section 3.1 and 3.2). In section 4.1 we present the field data and discuss them regarding the three mentioned gradients (section 4.2 surface characteristics; 4.3 topography and 4.4 macro-climate). These three gradients are important for the mountain permafrost distribution and the interpretation of its prediction (permafrost maps) in British Columbia.

2. Field sites and instrumentation

2.1. General site description

The macro-topography of British Columbia is characterized by two major mountain systems, the Coast Mountains and the Rocky Mountains, with plateaus and lesser ranges between them (Figure 1). Being at mid latitude (49°–60° N), within the west-drift zone, the general meridional orientation (NNW to SSE) of these mountain systems is responsible for

102 pronounced differences in climatic conditions between their coastal and continental sides.
103 Large gradients in precipitation and continentality (annual temperature amplitude for a
104 given latitude) characterize the climate of British Columbia (Figure 1). These differences
105 exist both at a macro-climatic scale with continentality increasing with distance from the
106 Pacific Ocean, and also at a meso-scale with orographic effects such as pronounced
107 temperature inversions in the interior valleys. Hence, an extreme west-east precipitation
108 gradient exists in the Coast Mountains and continentality is particularly pronounced at
109 lower elevations in, and east of, the Rocky Mountains (Wang et al. 2012).

110 The seven field sites of this study are located in northern BC between 54°45' and 59°
111 North. One is in the Coast Mountains (HUD: Hudson Bay Mtn.), two are in the Rocky
112 Mountains (NON: Nonda, POP: Poplars) and four are at the occidental edge of the Rocky
113 Mountains (GUN: Mt. Gunnel, TET: Tetsa, PIN: Pink Mountain, MID: Middlefork) (Figure
114 1). HUD, NON, GUN and PIN are high elevation sites, which means they are above the tree
115 line and at or near mountain tops while the other sites are below tree line and close to the
116 valley floor, or in relatively flat areas. The climate at the field sites, ranges from moderate-
117 humid alpine (Coast Mts.) to subarctic-continental (low-land north-eastern BC). The
118 mean annual air temperature (MAAT) at all sites is in the range of -5 to +1°C (Wang et al.
119 2012), hence all sites lie close to the climatic boundary for permafrost to exist.

120 The Nonda (1670 m ASL), Pink Mountain (1750 m ASL), and Hudson Bay Mountain
121 sites (~ 1950 -2150 m ASL) are clearly within the Alpine Tundra biogeoclimatic zone
122 (Meidinger and Pojar 1991) above treeline. The Mount Gunnel sites (1470 m ASL) are at
123 the lower boundary of the Alpine Tundra zone, above treeline, but transitioning into the
124 forested Black and White Boreal Spruce zone. With the exception of Hudson Bay
125 Mountain, all of these alpine sites are strongly windswept, resulting in very little snow
126 cover.

127 The remaining sites occur well within forested biogeoclimatic zones. The Middlefork
128 cluster (1000 m) is in the White Boreal Spruce zone, but includes a permafrost-underlain
129 peat plateau (dominated by *Sphagnum* and a sparse cover of black spruce (*Picea mariana*)),
130 a treeless cold air drainage meadow, and a zonal forest of white spruce (*Picea glauca*) and
131 aspen (*Populus tremuloides*). The Poplars (750 – 940 m ASL) and Tetsa (1000 m ASL)
132 sites are forested and fall within the Spruce Willow Birch zone. Both are instrumented
133 along elevation gradients on north and south facing exposures. There is striking aspect
134 control on vegetation here. South-facing slopes host trembling aspen (*Populus tremuloides*)
135 and lodgepole pine (*Pinus contorta*) and may have a grassy understory. Forest floors have
136 relatively thin humus forms. North-facing slopes tend to have a sparse cover of black spruce
137 (*Picea mariana*) and very thick mor (mossy) humus forms. In the latter forest type,
138 permafrost can usually be found some 60 cm below the forest floor.
139 Using instrumental data from nearby Environment Canada weather stations, climate
140 trends (1912-2003) for the region containing the Hudson Bay Mountain field site have
141 increased significantly by 0.8°C in mean annual air temperature (MAAT) (Egginton, 2005).
142 Climate trends (1937-2003) for the region containing the remaining field sites in north-east
143 BC have a statistically significant increase of 1.3°C in MAAT, 3.3°C significant increase in
144 extreme minimum temperature, and a 42% significant decrease in winter precipitation
145 (Egginton, 2005). The large part of this warming trend occurred between 1970 and 1990. A
146 brief analysis with updated time series from two Environment Canada weather stations in
147 the two regions shows no further warming trend in MAAT for the last two decades (1991 –
148 2012). For the observation period (2008 – 2012), the *Water supply and snow survey bulletin*
149 shows snow indices in the range of 75% to 140% from the long term mean (1981 – 2010) in
150 the two regions closest to our field sites (River Forecast Center, 2012a, 2012b).

2.2. Measurement parameters and instrumentation

The seven field sites vary regarding the sampling of the local conditions (topographic situation and surface characteristics) and so does the measurement setup. This non-standardised and not strictly systematic design is on one side due to absence / presence of various local conditions between field sites: E.g. steep bedrock is present only at some high-elevation sites whereas surface characteristics such as thick moss layers or forests are not present there (Table 1). On the other hand, some parameters are challenging to obtain and of limited use due to extreme small-scale variability (e.g. air temperature in rock faces or direct radiation in forests). The distance between individual measurement locations ranges from some decametres (e.g. GUN and NON site) to a few kilometers (low elevation sites POP, TET, and MID). For these reasons meteorological parameters are measured at one central location (wx) per high elevation site. The low elevation sites have air temperature measurements at each location similar to the setup of comparable studies in north-western Canada (Karunaratne and Burn, 2003).

The measured parameters are the temperature of the air (T_{air}), the ground-surface (GST or T_{surf}), and the ground (T_{ground}). The ground temperatures are sensed at a depth between 0.3 and 1.3 m for soils and debris, but at 0.1 m depth for bedrock. At the central weather stations (*wx*) other parameters such as rainfall, relative humidity, direct short wave irradiation, wind direction and speed, and barometric pressure are measured but used only as supplementary information in the present analysis. The weather stations are Onset *Hobo Weather Station* (H-21 or U30) and air temperature is measured in a solar radiation shield at 1.4 m above ground with a *S-THB-M002 Temperature/RH Smart Sensor (Tempcon),* which provides an accuracy of ±0.2°C above 0°C and ±0.4°C above –30°C. The other temperatures are recorded with *Hobo U23 pro V2* 2-channel mini loggers (*Onset*) which provide a similar accuracy. For air temperature the external sensors of the mini loggers are shielded with a similar radiation shield at 1.4 m height. Ground surface temperature is

177 usually recorded with the internal temperature sensor of the mini logger, which is buried a
178 few centimeters in the organic layer or debris, to minimize albedo effects. For near-surface
179 rock temperatures an external sensor is placed in a small hammer-drilled hole and sealed
180 with silicon glue. Physical disturbances (e.g. radiation influence of air temperature) are
181 assumed to be below the sensor accuracy (cf. Nakamura and Mahrt, 2005) on the level of
182 daily aggregates and even smaller for annual mean. Temperatures are sensed at 4 minute
183 sample intervals and aggregated and stored to hourly values.

184 The field sites selected and the sampling of local conditions, reflect the focus on
185 mountain permafrost. Gradients in hydrological conditions (wetlands, peats etc.) are barely
186 considered in this study despite their important role for the permafrost distribution in low-
187 land areas. Further, detailed air temperature and surface temperature lapse rates, which are
188 important for permafrost in valley bottoms in the very north of BC (Lewkowicz and
189 Bonnaventure, 2011), can not be extracted from our data (but a brief comparison of nearby
190 high and low elevation sites indicates pronounced winter inversions). Table 1 summarizes
191 the topographic situations and surface characteristics of the 41 locations with ground
192 temperature measurements and the three weather stations analysed in this study. In the
193 discussion section (4.2) we will refer to these local conditions in more detail.

194 ## 3. Data processing and analysis methods

195 ### 3.1. Pre-processing of raw temperature time series

196 At the field sites MID, NON, and POP measurements were initiated in summer 2007,
197 whereas, data acquisition started in 2008 for the other field sites. The data time series for
198 this analysis were retrieved between summer 2011 and 2013 for the last time. In the
199 supporting material a detailed description of filtering and an overview of the data
200 completeness is given. The filtering produces gaps of different characteristics: a) automated
201 filtering of invalid/corrupted values (not numeric or out of realistic range) cause short gaps

(single values); b) manual filtering of values from broken sensors (e.g. water damage or cable disruption) are applied over long time periods and cause long gaps (weeks to months). Because of these gaps it is not possible to directly compare all time series and simply calculate annual means for the same years. To account for this data characteristic we applied the processing described in section 3.2.

For all the data analysed in this study there is at least one continuous year of valid data. One exception is the air temperature measurement of the weather station at Mt. Gunnel. The very good correlation of 11 months existing data with the surface temperature recorded in a near-by rock cleft allow a reliable estimation of the mean annual air temperatures (c.f. supporting material).

3.2. Calculation of mean annual temperatures and their inter-comparability

Annual means of temperature time series (MAT) depend on the averaging period and the completeness of the raw data. Surface and thermal offsets, the differences between such annual means, are sensitive to errors in this mean calculation caused by data gaps. The surface offset (SO) has a pronounced inter-annual variability at locations with variable snow conditions. To minimize errors introduced by the data aggregation and to avoid misinterpretations of the resulting offsets due to temporal variations, we conduct the following processing steps: 1. Calculate daily mean temperature; 2. Calculate running mean annual temperature; 3. MAT, SO and TO statistics.

The hourly data is aggregated to *daily means*. Gaps up to two missing values per day are interpolated if more values are missing no daily mean is calculated.

Then, *running mean annual temperatures* (running MAT) are calculated for a 365 day window with 99% of data available (Figure 2a, c). Where sufficient data is present the offsets (SO, TO) for each point in time can be directly calculated and the minimum and maximum offset (e.g. SO_{min}, SO_{max} in Figure 2a) are subtracted and the measurement error

(±0.3°C) is added to get a measure of the uncertainty of the SO. This SO uncertainty is expressed with the spread in Figure 2b).

The example of Pink Mountain (Figure 2c) illustrates possible problems with the inter-comparability of annual means if time series are incomplete or if the running means are asynchronous: MATs from different points in time cannot be easily compared and offsets between running MATs vary strongly for some locations. This is considered with the next step of the data processing, which is described in detail in the supplementary material or in the discussion paper of this article (Hasler et al., 2014).

For the Hudson Bay Mountain field site, where the air temperature is measured at a weather station at 300m to 500m lower elevation (Table 1), an air temperature lapse rate of –5 ±1.25 °C/km is used for the calculation of the mean annual air temperature (MAAT), the SO and its uncertainty. For the *MAT, SO and TO statistics* the mean and the spreads (min.- and max.-values) of all running MAT values are calculated for each measurement variable. For short running MAT time series (below 50% of available data), the means and spreads are corrected by using a longer time series as a reference. As a reference the running MAT time series from the same field site with the best correlation during the overlapping time period is chosen (e.g. *cx_Tsurf* for *wx_Tair* in Figure 2c). The spreads are up scaled be the amount of variance that is captured by the overlapping period compared with the total variance of the running MAT time series. This results in a larger spread for shorter time series (cf. MAT of the air temperature *wx_Tair* in Figure 2c; this spread of ±1.4°C corresponds the variation of MAAT in the last two decades). In Figure 2d an example of a temperature profile shows the SO and TO at one location at Pink Mountain. In the further analysis, offsets are treated as significant (solid lines) if they are larger than the (inner) half of the uncertainties of both considered MATs. The uncertainty of the offset is indicated by the spreads in Figure 2d. This calculation of mean annual temperatures and the conservative

estimate of the uncertainties allows a comparison of inconsistent data for a "quasi-static" surface offset- / thermal offset- analysis.

3.3. Annual temperature amplitudes and seasonal N-factors

The annual temperature amplitudes used in this article are the differences between mean July and mean January temperatures divided by 2. The N-factors used in the discussion of the snow cover influence are calculated on a seasonal and biweekly (15-days) basis by dividing the freezing or thawing index of the surface by the respective index of the air temperature (If_{surf} / If_{air} or It_{surf} / It_{air}). For seasonal indices and N-factors only days with complete data (T_{air} and GST present) are considered. The distinction between thawing and freezing season is made by the 15-days running average air temperature ($T_{air} \geq 0°C$ is thawing season; $T_{air} < °C$ is freezing season). Whereas other studies (cf. Karunaratne and Burn, 2003) used the cumulative index since the start of the season, the biweekly integration shows the contribution of each time period to the seasonal n-factor with similar weight. The 15-days averaging window is chosen for optimal visual representation but a slightly shorter or longer window (3 – 30 days) has similar results. Because the relative errors of all these calculations are much smaller than for the SO and TO calculation, we do not detail their uncertainties here.

4. Results and discussion

4.1. Overview of the mean annual temperatures and offsets

Figure 3 gives an overview of all mean annual temperature (MAT) profiles and the significance of the surface and thermal offsets (SO, TO). For all locations with snow accumulation (non-vertical), the SO has a temporal variability depending on the snow cover

277 evolution. Because the observation period covers years with different snow cover build-up
278 (cf. section 2.1), these few years cover a large part of the variability in SO of the last 30
279 years. However, the particular situation for one location considering snow redistribution
280 effects and data gaps does not allow to precisely quantify the SO and its uncertainty.
281 Therefore the estimation of the uncertainty is very conservative (section 3.2) and SOs
282 indicated as significant (solid lines in Figure 3) are likely to prevail for most of the last 30
283 years. The TOs are often not significant due to their small offset or due to a pronounced
284 variability because the lower ground is isothermal at 0°C but not the ground surface (cf.
285 Poplars in Figure 3). These isothermal conditions are discussed in section 4.2.

286 All sites show MAATs below zero degrees Celsius except south facing slope at Poplars
287 *(POP_S),* which has a particularly warm micro-climate (Figure 3). In contrast, half of the
288 locations show positive mean annual ground and ground surface temperatures (MAGT,
289 MAGST). Hence, the SOs are generally positive and range from 0.5°C to 7°C. The TOs
290 (thermal offsets or "temperature offsets in the near-surface" where the ground temperature
291 is measured above the permafrost table) are often not significant and range from -2°C to
292 +1°C.

293 The SOs are important for permafrost distribution and dominate the effects of TOs in
294 these climatic conditions and surface types (mountain permafrost). In the following, the
295 results, and in particular the surface offsets, are presented and discussed regarding
296 variations in surface characteristics, topography and macro-climate which may be related to
297 the micro-, meso-, and macro-scale (Gruber, 2012). The variation in the parameters of
298 interest (surface type, snow accumulation, slope, aspect, elevation, macro-climate etc.) is
299 not sufficiently systematic and the sample is too small to quantify the difference in the
300 offsets along all potential gradients with statistical methods. Accordingly, the approach we
301 use is an exemplary comparison of the offsets at locations that differ mainly in the
302 parameter of interest but are as similar as possible in the other parameters.

4.2. Surface and thermal offsets classified by surface characteristics

First, we discuss the offsets of the mean annual temperatures regarding different *surface characteristics*. With surface characteristics we denote classes of near-surface ground properties (*surface type*), micro-topography and vegetation cover regarding their thermal influence. A brief description of surface characteristics for all measurement locations is given in Table 1 in the columns *surface type* and *note*. These characteristics can vary over short distances and are responsible for a pronounced small-scale variability of ground temperatures (Gubler et al., 2011; Gisnås et al., 2014); however, their degree of influence may vary between sites with different macro-climatic conditions. In this section we quantify the effect of different surface characteristics on the surface and thermal offset (SO, TO) at our field sites. Even if the sample is too small and not systematic, as described above, we get a first estimate of the influence of surface characteristics on permafrost occurrence in British Columbia and compare these influences between sites.

Figure 4 shows the SO and TO of all locations ordered by surface characteristics based on a simple classification. We distinguish the following first order classes: *rock, soil, debris,* and *forest.* The class *rock* comprises near-vertical bedrock at different aspects and flat bare rock. Under *soil* we include fine-grained substrate (mineral soils and colluvium) with minor vegetation such as alpine tundra at Nonda and Pink Mountain *(NON, PIN)* or herbaceous meadows at Middlefork *(MID_wx)*. The class *debris* contains all surfaces with coarse debris cover that contain voids that may allow air circulation. Finally, *forest* comprises different forest types such as black spruce, pine and alder forests. These forests generally have mossy forest floors, overlying mineral soil horizons except as otherwise remarked (Figure 4). In addition to the first order classes of surface type, we collected meta data on the exposure to solar radiation and wind (Figure 4; top). These factors are influenced by the (micro-) topography and affect the snow deposition (wind) and the radiation balance (mainly insolation) when snow free.

329 In general the SOs on flat locations with snow cover is in the range of 0.5 to 3°C what
330 corresponds to similar settings in Southern Norway (Farbrot et al., 2011; Isaksen et al.,
331 2011). The average SO per class does not show a clear dependency on the surface type. For
332 comparable irradiation and wind (snow redistribution) conditions the SOs on flat bare rock
333 (2.5–4°C) appear to be slightly higher than for the other surface types, which are in the
334 range of 1.5 to 3°C (Figure 4). This difference may be caused by the low albedo of the rock
335 additionally to a bias due to slightly different snow cover influence. Interestingly, the SOs
336 on coarse debris are not significantly smaller than for the other surface types. Within the
337 first 30–50 cm of the block layer no significant offset (see TO) was observed. Obviously the
338 ventilation (Haeberli, 1973; Harris and Pedersen, 1998) and reduced thermal conductivity
339 (Gruber and Hoelzle, 2008) of the block layer have no large effect on the thermal regime of
340 our field sites, however, a part of the TO may be missed due to the shallow measurement
341 depth.
342 Within the class *near-vertical bedrock* a variation in the SOs of 4°C (SO: 1–5°C)
343 indicates the influence of aspect controlled irradiation on these snow free surfaces, which is
344 discussed in more detail in the next section. Note that for this class no rock temperature at
345 depth is measured, and that the near-surface temperature is used for the SO calculation
346 (Figure 4). In the classes *soil and debris*, which comprise more gentle slopes with snow
347 accumulation, the aspect control is smaller. The north-south difference of the SOs is about
348 2°C for the alpine tundra at Nonda (*NON_S* vs. *NON_N*) and 1.5 to 3°C in the coarse debris
349 at Hudson Bay Mountain (*HUD_scr1–5* in Figure 4). For coniferous forests with a dense
350 canopy (spruce, pine), where the SOs are approximately 2°C, there is no difference between
351 north and south slopes. However, the forest type, and correspondingly the canopy density,
352 may be influenced by the aspect. This leads to significantly larger SOs where light forest
353 and broadleaf trees allow higher incident solar radiation (e.g. *POP_S* in Figure 4).

354 Wind exposed locations with only a thin snow cover lead to a smaller SO than at
355 sheltered locations at all field sites. Whereas the SO at the three wind exposed locations in
356 the rock mountains is 1°C or less, the wind-swept location at Hudson Bay Mountain (*HUD*)
357 has an SO of 2.7°C (Figure 4). This larger offset may bee a result of more snow
358 accumulation at wind exposed locations of *HUD* due to more frequent warm snowfall in the
359 Coast Mountains. Similar surface offset (< 1°C) at wind-swept location have been reported
360 from norwegian mountain Permafrost sites (Farbrot et al., 2011).
361 Regarding the influence of vegetation and organic layer on SO and TO, the field sites
362 Middlefork and Poplars are of special interest. At Middlefork the weather station locations
363 in open meadow (*MID_wx*), a palsa in a light stand of black spruce (*MID_pf*), and a spruce
364 forest with closed canopy on a gentle slope (*MID_fr*) indicate a decrease in SO with
365 increasingly dense vegetation (Figure 4). Hence the lower air temperature at the locations
366 with lesser vegetation due to cold air drainage is overcompensated by these larger SOs (cf.
367 Figure 3). At the location with permafrost occurrence *MID_pf*, a clearly negative TO (–
368 1.3°C) is responsible for the permafrost occurrence (Figure 4). If this TO is caused by the
369 seasonally variable thermal conductivity of the moss layer (thermal diode) or by a transient
370 effect of the latent heat required to melt massive ice within the degrading palsa is not clear
371 based on this data alone. An additional cooling effect due to reduced snow depth on the
372 palsa usually described in the literature could not verified with our data because the smaller
373 SO on the palsa compared to weather station (*MID_wx*) is manly caused by summer
374 temperatures (perhaps shading from black spruce or different depth of probes). At the
375 Poplars field site a clearly larger SO in contrast to the other locations is observed at the
376 south slope location *POP_S* (Figure 4). This large SO is caused by warmer ground
377 temperatures in summer. Hence, the higher transmissivity of the aspen forest allows more
378 irradiative warming of the ground compared to the black spruce forest on the other
379 locations. The three locations with a thick (> 30 cm) moss layer in the northern slope of

Poplars (*POP_N1–3*) show significant TOs between –0.8 and –1.7°C. The ground temperatures of these locations are at 0°C throughout the year, similar to the palsa at Middlefork (*MID_pf*). Here as well, it is not clear whether these TOs reflect an equilibrium thermal offset effect of the organic soil layer or if they indicate degrading permafrost with high ice content (cf. Isaksen et al. 2011).

4.3. Aspect control of rock temperatures on the example of near-vertical cliffs

Near-vertical rock temperatures are a comparably good parameter to investigate the aspect control of ground temperatures and to validate radiation algorithms in physically based permafrost models because no complex surface characteristics, thermal offsets and snow complicate the situation (Gruber et al. 2004). Gruber (2012) points out the importance of an extension of existing measurements to other environmental conditions for a better understanding of the drivers of these temperatures. In this section we describe the surface offsets in steep bedrock at the three high elevation sites GUN, PIN, and HUD and discuss them in comparison to near-vertical rock temperatures in other regions.

The mean annual rock temperatures from the near-surface (MARST or MAGST) at Mt. Gunnel illustrate the aspect control of ground temperatures by solar irradiation. At the shaded north side (*GUN_N*) MAGST is just 0.9°C higher than MAAT whereas this SO on the south side (*GUN_S*) is approximately 5°C (Table 2). Subtracting these two north and south face SOs yields a difference of 4.1 °C. A significant east-west difference does not exist (cf. *GUN_E* and *GUN_W*, Table 2). The N-S difference at Hudson Bay Mt. (*HUD_S2* vs. *HUD_N*) is 3.8°C. If not caused by differences in albedo or sky view factor, the slightly smaller N-S difference at HUD may be related to the higher cloudiness at Hudson Bay Mt. common in the more humid Coast Mountains. However, the difference is too small (not significant; cf. uncertainty in Fig. 4) to draw any conclusions on this macro-climatic effect. The effects was neither detectible in other empirical studies (Gruber, 2012). For Pink

406 Mountain we cannot calculate the north-south difference because the corresponding aspects
407 are not monitored. The SO values from the south-east and west cliff (*PIN-SE* and *PIN-W*)
408 correspond with similar aspects at Mt. Gunnel.

409 Compared with near-vertical rock temperatures in other mountain ranges, this influence
410 of aspect falls between the values reported for mid-latitudes (Swiss and New Zealand Alps)
411 and slightly higher latitudes (Norway). In the Swiss Alps N-S differences from 6 to 8°C are
412 reported (Gruber et al., 2004; PERMOS, 2010; Hasler et al., 2011), in New Zealand this
413 difference is about 6°C (Allen et al. 2009), whereas in middle Norway differences of 3 to
414 3.5°C were observed (Hipp et al., 2014). Strong (directional) reflection in steep glacial
415 environments amplifies the short-wave incoming radiation on southern rock faces (Allen et
416 al. 2009; Hasler et al., 2011) and makes the high values not directly comparable to the
417 situation in this study. A stronger decay of the expositional difference of PISR occurs north
418 of about 60° N (Gruber, 2012) where expositional differences in the range of 0.5 to 1.5°C
419 are reported at 80°N (Lewkowicz, 2001).

420 Within compact bedrock, thermal offset effects are small and rock surface temperatures
421 are a reasonable assumption to extrapolate (permafrost) temperature at depth. However,
422 micro-topographic influences such as snow retention on ledges and air ventilation in
423 fractures influence the subsurface temperature field (Hasler et al., 2011). In the case of Mt.
424 Gunnel the MAGST of the shadowy rock faces, the large fracture and the top surface is
425 slightly below 0°C whereas the other free surfaces have annual means above 0°C. Hence,
426 the micro-topography is essential for permafrost estimates at Mt. Gunnel. Warm permafrost
427 is only expected in the following settings: below steep north faces, in fractured rock, under
428 blocky layers and under wind-swept surfaces. Compact rock in E–S–W aspects and surfaces
429 with snow accumulation (center of plateaus, forest) are unlikely to contain permafrost.
430 Hence, the rock fall that occurred at Mt. Gunnel and the near-by Vanessa rock slide
431 (Geertsema and Cruden, 2009) are possibly related to such local permafrost occurrence.

4.4. The influence of continentality on snow cover-induced surface offsets

Total annual precipitation, annual air temperature amplitude and average cloud-cover are highly correlated on the large scale and distinguish humid maritime and dry continental climates (cf. section 2). Continentality is usually defined as annual air temperature amplitude for a given latitude or simply half of the difference of January and July air temperature (cf. section 3.3). With increasing continentality less (winter) precipitation and, on average, a thinner snow cover is expected. Even though snow can have diverse cooling and warming effects, one of its major impacts is the thermal insulation of the ground from winter air temperature (Zhang, 2005). This affects the *nival offset*, that part of the SO which is caused by insulation of the snow cover and which is considered in N-factor models (e.g. Smith and Riseborough, 2002). However, the correlation between mean snow cover thickness and annual air temperature amplitude on the macro-scale makes it difficult to predict how the SO depends on continentality. Additionally, the variability in snow cover persistence further complicates the situation.

Because our measurements span large gradients in continentality (cf. section 2.1), they provide an opportunity to directly evaluate the effect of continentality on SO (with field measurements of similar characteristics) and to estimate its role for the permafrost distribution in British Columbia. Generally, the measured annual air temperature amplitude and the precipitation sum (Wang et al. 2012) correlate negatively with each other, however, the high elevation site in the inner Rocky Mountains (e.g. Nonda) shows a comparably low precipitation sum but rather small annual air temperature amplitudes.

The aggregated data per field site shows no clear difference between Coast Range and continental (East) side of the Rocky Mountains in terms of SOs (Figure 5). Because the mean surface offsets per site are biased by the surface characteristics, the missing dependency on this aggregation level is not surprising. However, locations from the same surface class do not show a consistent dependency on either the annual air temperature

458 amplitude, nor on the annual precipitation (Figure 5) because they are not present at all sites
459 and topographic effects (radiation and local snow redistribution) lead to strong variability
460 within these classes (cf. section 4.2).

461 To further investigate the nival offset and the effect of snow cover persistence on the
462 surface offset, single locations with similar characteristics but different macro-climate are
463 compared. A first example is the comparison of a location at Hudson Bay Mountain with
464 one at Middlefork (Figure 6). Both locations accumulate snow without much influence of
465 wind. The site *HUD_fl* is a near-horizontal rock surface on the south slope of Hudson Bay
466 Mtn. with a thick winter snow cover. In contrast, *MID_wx* is located on a very gentle
467 sloping meadow overlying till (fine-grained soil). Like *HUD_fl, MID_wx* also has no
468 particular shading or wind influence (cf. Table 1), but it has a much drier and more
469 continental climate. The MAAT at both locations is around -3°C and the influence of
470 differences in moisture content (soil vs. bedrock) is apparently not affecting the surface
471 temperature measurements (no significant zero curtain at the soil site). The temperature
472 difference shows clearly that the nival offset (orange area during winter in Figure 6; middle)
473 is larger in the case of *MID_wx* even though the ground surface is colder at this location
474 during winter. The seasonal N-factors at both sites correspond to the values observed for
475 thick snow cover (> 0.8m) in other studies (Smith and Riseborough, 2002; Juliussen and
476 Humlum, 2007). The seasonal and biweekly freezing N-factors (Figure 6; bottom *nf*) are
477 slightly smaller at *MID_wx*, indicating a less insulating snow cover. Despite this smaller
478 insulation, the effect of the larger annual air temperature amplitude augments the nival
479 offset. An additional difference between the temperature regimes at the two locations is
480 shown by the thawing N-factors (Figure 6; bottom *nt*). At *MID_wx*, where the entire
481 summer is snow free, *nt* is close to one, whereas at *HUD_fl* the snow cover persists until
482 August and leads to a strong reduction of *nt* likely by albedo and latent heat effects (cf.
483 Zhang 2005). The resulting negative summer offset at HUD (Figure 6 middle; blue area)

484 further reduces the SO. In this example the maritime humid climate leads to an SO of 3.9°C
485 due to a smaller temperature amplitude and a long-lasting snow cover while the drier
486 continental climate results in a SO of 6.1°C. A second example comparing two locations
487 with thin snow cover is given in Figure 7. These locations are a wind exposed scree slope at
488 Hudson Bay Mountain (*HUD_scr2*) and the wind-swept top of Mount Gunnel (*GUN_fl*). At
489 both sites the GST generally follows the air temperature, hence, the SOs and temperature
490 differences are relatively small and have a less pronounced seasonal pattern (Figure 7;
491 middle) and freezing N-factors closer to one than in the previous example (Figure 7;
492 bottom). A clear positive offset is caused at *HUD_scr2* in one winter (2010/2011) by a
493 more developed snow cover. At this location GSTs below air temperature can be observed
494 in early summer (blue areas in Figure 7; middle left). At *GUN_fl* a slightly positive
495 temperature difference persists throughout the thawing season (blue areas in Figure 7;
496 middle right). The related thawing N-factors (*nt*) are higher at the Gunnel location than at
497 *HUD_scr2* likely due to the effect of the short-wave radiation (cf. Juliussen and Humlum,
498 2007). Hence, the difference in annual temperature amplitude plays a minor role in this
499 example and the slight difference in snow cover thickness and duration affects both,
500 thawing and freezing N-factor and results in a just slightly higher SO at *HUD_scr2* (Figure
501 7). These two examples illustrate that several opposed effects tend to compensate each other
502 on the macro-climatic scale. A complete set of figures showing the temperature differences
503 and N-factors is contained in the supplementary material. The opposed effects become
504 small where the snow cover is eroded (but there SOs are small in general) and apparently
505 increase for snow rich local conditions (small nf but also reduced nt).

506 On these considerations we build the hypothesis, that the macro-climatic effect on snow-
507 cover induced SOs is much smaller than expected from local studies, where only the snow-
508 cover thickness varies but similar air temperature amplitudes force the heat fluxes (Figure
509 8). In Figure 8 we sketch the hypothetical SO variation based on local snow cover

variability (with constant annual air temperature amplitude) and based on a gradient in snow cover coinciding with a gradient in continentality such as the case in our study region (and other mid latitude mountain ranges). For a climatic range where a persistent winter snow cover builds up, the SO is larger in a continental climate and smaller in a maritime climate than the SOs of the same snow cover but intermediate air temperature amplitude (Figure 8). This may be important for the application of empirical mountain permafrost models over large areas with significant macro-climatic variations. A further consequence from the dependency shown in Figure 8 is the strong sensitivity on snow cover variations and temporal changes for continental climates due to the large annual air temperature amplitude.

5. Conclusion

This study comprises the analysis of an extensive data set of near-surface ground temperatures that is novel for the province of British Columbia. Despite the heterogeneous data characteristics, "quasi-static" values for the surface and thermal offsets could be achieved. The main focus of the paper is to analyse the surface offset and thermal offsets regarding the three groups of influencing factors *surface characteristics*, *topography* and *macro-climate.* The respective key findings are listed separately as follows:

Surface characteristics:

- In our measurements the average of the surface offsets per class of surface type (rock, fine soil, coarse debris, forest) is 2 to 2.5°C with no clear difference between classes.
- Most wind-swept surfaces show a smaller surface offset (below 1°C). In one case the offset is larger, possibly due to more frequent wet snowfall.
- The observable surface offsets on coarse blocky material are similar to the ones in fine-grained material.

- Thermal offsets or offsets in the near-surface layer are negligible in our measurements, except at north facing forest sites with a thick organic layer (moss) they are –1 to –2°C. It is not clear if these latter thermal offsets represent equilibrium conditions because the temperature at the permafrost table is constantly at 0°C and transient effects may be important under such conditions. This study only included one wetland (with peat) due to its focus in mountain permafrost.

Aspect control of insolation

- The north-south difference of the surface offset in near-vertical bedrock is 4°C. No east-west difference was detected.
- On gentle slopes (angle < 30°) on alpine tundra or debris the observed north-south difference is between 1.5°C and 3°C. In forests with a dense canopy this difference is negligible.

Macro-climate

- The aspect control of the surface offset in steep bedrock does not show significant differences between different macro-climatic regions.
- The comparison of two locations with a thick snow cover indicates that the effect of snow cover insulation (nival offset) in the humid Coast Mountains and the much drier occidental side of the Rocky Mountains is similar for locations. This is due to the reverse effect of the continentality (annual air temperature amplitude), which compensates for the decreased insulation (smaller freezing N-factor) with lower winter temperatures (larger freezing index) in the continental climate.
- At the site in the Coast Mountains the long-lasting snow cover further reduces the surface offset by albedo and latent heat effects during early summer.

Regarding future estimates of permafrost distribution in British Columbia, local variability of the surface offset caused by topographic and micro-topographic effects is most important. This variability differs with vegetation and organic soil layers (which also

560 controls the thermal offset) but seems to be influenced only to minor extent by the macro-
561 climatic variations.

562 **Author contributions**

563 M. Geertsema, V. Foord, and S. Gruber designed, deployed and maintained the field
564 measurements of the present study. A. Hasler performed the data analysis. J. Noetzli
565 contributed data processing routines as well as the numerical model in the discussion paper.
566 A. Hasler prepared the manuscript with contributions and editing of all co-authors.

567 **Acknowledgements**

568 Thanks to two anonymous reviewers for their useful comments that helped to improve the
569 manuscript! Further we would like to thank Hudson Stoffels for his active support in the
570 field campaigns.

References

Allen, S. K., Gruber, S., and Owens, I. F.: Exploring steep bedrock permafrost and its relation- ship with recent slope failures in the Southern Alps of New Zealand, Permafrost Periglac., 20, 345–356, 2009.

Boeckli, L., Brenning, A., Gruber, S., and Noetzli, J.: A statistical approach to modelling permafrost distribution in the European Alps or similar mountain ranges, The Cryosphere, 6, 125–140, doi:10.5194/tc-6-125-2012, 2012.

Bonnaventure, P. P., Lewkowicz, A. G., Kremer, M., and Sawada, M. C.: A permafrost probability model for the southern Yukon and northern British Columbia, Canada, Permafrost Periglac., 23, 52–68, 2012.

Cermak, V. and Rybach, L.: Thermal conductivity and specific heat of minerals and rocks, Landolt-Bornstein, Zahlenwerte and Funktionen aus Naturwissenschaften and Technik, 305– 343, 1982.

Egginton, V. N.: Historical climate variability from the instrumental record in northern British Columbia and its influence on slope stability, Department of Earth Sciences – Simon Fraser University, 2005.

Farbrot, H., Hipp, T.F., Etzelmüller, B., Isaksen, K., Ødegård, R.S., Schuler, T.V., und Humlum, O.: Air and ground temperature variations observed along elevation and continentality gradients in Southern Norway. Permafrost Periglac., 22, S,343–360, 2011.

Fiddes, J. and Gruber, S.: TopoSCALE v.1.0: downscaling gridded climate data in complex terrain, Geosci. Model Dev., 7, 387–405, doi:10.5194/gmd-7-387-2014, 2014.

Geertsema, M. and Cruden, D. M.: Rock movements in northeastern British Columbia, in: Landslide Processes: From Geomorphologic Mapping to Dynamic Modelling, Proceedings of the Landslide Processes Conference: a tribute to Theo van Asch, edited by: Malet, J. P., Remaitre, A., Bogaard, T., Strasbourg, 6–7 February, CERG, Strasbourg, France, 31–36, 2009.

Geertsema, M., Clague, J. J., Schwab, J. W., and Evans, S. G.: An overview of recent large catastrophic landslides in northern British Columbia, Canada, Eng. Geol., 83, 120–143, 2006.

Gisnås, K., Westermann, S., Schuler, T.V., Litherland, T., Isaksen, K., Boike, J., and Etzelmüller, B.: A statistical approach to represent small-scale variability of permafrost temperatures due to snow cover. The Cryosphere, 8, 2063–2074, doi: 10.5194/tc-8-2063-2014, 2014.

Gruber, S.: A Global view on permafrost in steep bedrock, in: Proceedings of the 10th International Conference on Permafrost, Salekhard, Russia, 25–29 June 2012, 131–136, 2012

Gruber, S. and Hoelzle, M.: The cooling effect of coarse blocks revisited: a Modeling Study of a Purely Conductive Mechanism, in: Proceedings of the Ninth International Conference on Permafrost, Fairbanks, Alaska, USA, 29 June–3 July 2008, 557–561, 2008.

Gruber, S., Hoelzle, M., and Haeberli, W.: Rock-wall temperatures in the Alps: modelling their topographic distribution and regional differences, Permafrost Periglac., 15, 299–307, 2004.

Gubler, S., Fiddes, J., Keller, M., and Gruber, S.: Scale-dependent measurement and analysis of ground surface temperature variability in alpine terrain, The Cryosphere, 5, 431–443, doi:10.5194/tc-5-431-2011, 2011.

Guodong, C. and Dramis, F.: Distribution of mountain permafrost and climate, Permafrost Periglac., 3, 83–91, 1992.

Haeberli, W.: Die Basis-Temperatur der winterlichen Schneedecke als möglicher Indikator für die Verbreitung von Permafrost in den Alpen, Zeitschrift für Gletscherkunde and Glazialgeologie, 9, 221–227, 1973.

Harris, C., Arenson, L. U., Christiansen, H. H., Etzelmüller, B., Frauenfelder, R., Gruber, S., Haeberli, W., Hauck, C., Hölzle, M., and Humlum, O.: Permafrost and climate in Europe: Monitoring and modelling thermal, geomorphological and geotechnical responses, Earth-Sci. Rev., 92, 117–171, 2009.

Harris, S. A.: Permafrost distribution, zonation and stability along the eastern ranges of the cordillera of North America, Arctic, 39, 29–38, 1986.

624 Harris, S. A.: Continentality Index: Its uses and limitations applied to permafrost in the Canadian
625 Cordillera, Physi. Geogr., 10, 270–284, 1989.
626 Harris, S. A.: Climatic change and permafrost stability in the eastern Canadian Cordillera, in:
627 Extended Abstracts of the Ninth International Conference on Permafrost, Fairbanks, Alaska,
628 USA, 29 June–3 July 2008, 93–94, 2008
629 Harris, S. A. and Pedersen, D. E.: Thermal regimes beneath coarse blocky materials, Permafrost
630 Periglac., 9, 107–120, 1998.
631 Hasler, A., Geertsema, M., Foord, V., Gruber, S., und Noetzli, J.: The influence of surface
632 characteristics, topography, and continentality on mountain permafrost in British Columbia.
633 The Cryosphere Discussions, 8, S,4779–4822, doi: 10.5194/tcd-8-4779-2014, 2014.
634 Hasler, A., Gruber, S., and Haeberli, W.: Temperature variability and offset in steep alpine rock and
635 ice faces, The Cryosphere, 5, 977–988, doi:10.5194/tc-5-977-2011, 2011.
636 Hipp, T., Etzelmüller, B., and Westermann, S.: Permafrost in alpine rock faces from Jotunheimen
637 and Hurrungane, Southern Norway, Permafrost Periglac., 25, 1–13, 2014.
638 Isaksen, K., Ødegård, R.S., Etzelmüller, B., Hilbich, C., Hauck, C., Farbrot, H., Eiken, T., Hygen,
639 H.O., und Hipp, T.F.: Degrading Mountain Permafrost in Southern Norway: Spatial and
640 Temporal Variability of Mean Ground Temperatures, 1999–2009. Permafrost Periglac., 22,
641 361–377, 2011.
642 Juliussen, H. and Humlum, O.: Towards a TTOP ground temperature model for mountainous terrain
643 in central-eastern Norway. Permafrost Periglac., 18, 161—184, 2007.
644 Karunaratne, K. C. and Burn, C. R.: Freezing *n* factors in discontinuous permafrost terrain, Takhini
645 River, Yukon Territory, Canada, in: Proceedings of the 8th International Conference on
646 Permafrost, Zurich, University of Zurich-Irchel. S., 519–524, 2003.
647 King, L.: Zonation and ecology of high mountain permafrost in Scandinavia, Geogr. Ann. A, 131–
648 139, 1986.
649 Lewkowicz, A. G.: Temperature regime of a small sandstone tor, latitude 80◦ N, Ellesmere Is- land,
650 Nunavut, Canada, Permafrost Periglac., 12, 351–366, 2001.
651 Lewkowicz, A. G. and Bonnaventure, P. P.: Equivalent elevation: a new method to incorporate
652 variable surface lapse rates into mountain permafrost modelling, Permafrost Periglac., 22,
653 153–162, 2011.
654 Lunardini, V.: Theory of *n* factors and correlation of data, in: Proceedings of the Third Inter-
655 national Conference on Permafrost, Edmonton, Alberta, Canada, 10–13 July 1978, 40–46,
656 1978
657 Mottaghy, D. and Rath, V.: Latent heat effects in subsurface heat transport modelling and their
658 impact on palaeotemperature reconstructions, Geophys. J. Int., 164, 236–245, 2006.
659 Nakamura, R. and Mahrt, L.: Air temperature measurement errors in naturally ventilated radia- tion
660 shields, J. Atmos. Ocean. Tech., 22, 1046–1058, 2005.
661 Noetzli, J. and Gruber, S.: Transient thermal effects in Alpine permafrost, The Cryosphere, 3, 85–
662 99, doi:10.5194/tc-3-85-2009, 2009.
663 PERMOS: Permafrost in Switzerland 2006/2007 and 2007/2008, Glaciological Report (Per-
664 mafrost) No. 8/9, edited by: Noetzli, J. and Vonder Muehll, D., Cryospheric Commission of
665 the Swiss Academy of Sciences, Zurich, Switzerland, 2010.
666 Riseborough, D., Shiklomanov, N., Etzelmuller, B., Gruber, S., and Marchenko, S.: Recent ad-
667 vances in permafrost modelling, Permafrost Periglac., 19, 137–156, 2008.
668 River Forecast Center: Water supply and snow survey bulletin – January 1st, 2012, available at:
669 http://bcrfc.env.gov.bc.ca/bulletins/watersupply/archive/2012/2012_Jan1_SnowBulletin.pdf,
670 2012a.
671 River Forecast Center: Water supply and snow survey bulletin – April 1st, 2012, available at:
672 http://bcrfc.env.gov.bc.ca/bulletins/watersupply/archive/2012/2012_Apr1_SnowBulletin.pdf
673 , 2012b.
674 Schneider, S., Hoelzle, M., and Hauck, C.: Influence of surface and subsurface heterogeneity on
675 observed borehole temperatures at a mountain permafrost site in the Upper Engadine, Swiss
676 Alps, The Cryosphere, 6, 517–531, doi:10.5194/tc-6-517-2012, 2012.
677 Smith, M. W. and Riseborough, D. W.: Climate and the limits of permafrost: a zonal analysis,
678 Permafrost Periglac., 13, 1–15, 2002.

679 Throop, J., Lewkowicz, A. G., Smith, S. L., and Burn, C. R.: Climate and ground temperature re-
680 lations at sites across the continuous and discontinuous permafrost zones, northern Canada,
681 Can. J. Earth Sci., 49, 865–876, 2012.
682 Wang, T., Hamann, A., Spittlehouse, D. L., and Murdock, T. Q.: ClimateWNA-High-resolution
683 spatial climate data for western North America, J. Appl. Meteorol. Clim., 51, 16–29, 2012.
684 Zhang, T.: Influence of the seasonal snow cover on the ground thermal regime: an overview, Rev.
685 Geophys., 43, RG4002, doi:10.1029/2004RG000157, 2005.
686
687

Figure captions

Figure 1: Overview of the field sites on a precipitation map of British Columbia. The field sites span a latitudenal range from 54°45' to 59°N and are located within or close to the Coast Mountains and Rocky Mountains. These two main mountain ranges cause large gradients in precipitation and continentality within short distance (precipitation data from Wang et al. 2012).

Figure 2: The running mean annual temperatures (running MAT) at two field sites and two profile plots of the MAT. a): Mt. Gunnel. All near-surface MAT from vertical rock faces have a development parallel to the mean annual air temperature (MAAT). Indications of maximum and minimum surface offset are explained in text. b) example of the surface offset (SO) shown in the MAT profile of a west facing cliff at Mt. Gunnel. The temperature at 1.4 m height is the MAAT. c): Pink Mountain. The MAT from convex (cx) and concave (cc) landforms show inverse development. Offsets strongly depend on the point in time of the comparison of instantaneous MATs. This example is a worst case in terms of data completeness. d): MAT profile with spreads indicating the uncertainties of the surface- and thermal offsets at Pink Mt. The solid lines indicates an offset that is larger than the spread (TO), the dashed line is used if offset is equal or smaller than the spread (SO).

Figure 3: Overview of all thermal profiles measured at 44 locations within the seven field sites. The temperatures at 1.4 m height are the mean annual air temperatures (MAAT). Dashed lines indicate offsets below the inward uncertainty (Offset < U_{offset} / 2) of these offsets (section 3.2). Solid lines indicate significant offsets.

Figure 4: Surface and thermal offsets grouped by different surface types (substrate and vegetation) and with indication of micro-topographic situation and forest type.

Figure 5: Surface offsets (SO) against macro-climatic parameters. Large symbols are means per site and small symbols are individual locations with symbol given by surface type. Left: SO against measured annual amplitude of air temperature (ATA = ($T_{july} - T_{jan}$)/2); right: SO against annual precipitation sum (precipitation estimate from Wang et al. 2012).

Figure 6: Seasonal development of temperature differences and N-factors at flat rock on Hudson Bay Mt. (left) and in a flat meadow at Middlefork (right). Top: air and ground surface temperature (15-days running mean); middle: temperature difference (GST–T_{air}) on 15-days running average; bottom: N-factors on seasonal average (bars) and 15-days average (points). The SO is to one part controlled by the winter air temperature and is larger at MID_wx (orange area; middle). Negative differences in early summer (blue area; middle left) contribute to a smaller SO at HUD_fl. Freezing N-factors (*nf*) are on a similar level (0.1–0.2), whereas thawing N-factors (*nt*) differ due to the persistence of the snow during summer at HUD_fl.

Figure 7: Seasonal development of temperature differences and N-factors in a windy scree slope at Hudson Bay Mt. (left) and on a windy plateau at Mt. Gunnel (right). Top: air and ground surface temperature (15-days running mean); middle: temperature difference (GST–T_{air}) on 15-days running average; bottom: N-factors on seasonal average (bars) and 15-days average (points). Note that the 2009 and 2011 seasonal thawing N-factors (*nt*) at *HUD_scr2* are slightly biased by the incomplete data. At both sites GST follows the air temperature. The snow cover is slightly more developed at *HUD_scr2* and reduces both, freezing and thawing N-factor.

Figure 8: Qualitative sketch of the effect of snow cover and continentality on the surface offset (SO): The dashed red line indicates the dependency on a macro-climatic continentality gradient (annual air temperature amplitude) correlated with an increase in precipitation (and snow thickness; strong seasonality of precipitation is neglected). The black line corresponds to the effect of local variations in snow accumulation (wind drift etc.) but constant annual air temperature amplitude. While SO increases with snow cover thickness for local variations until the effect of snow persistence reverses the trend, the continentality effect leads to a small variation of the SO for conditions with a seasonal snow cover.

Tables

Table 1: Measurement locations at all field sites. Locations with common parameters are summarized.

site	*location*[1]	*elevation* (m a.s.l.)	*slope* (°)	*aspect* (°)	*surface type*	*note*
GUN	wx	1470	0	-		no ground T
GUN	cr	1470	90	240	rock cleft	no snow
GUN	N, E, S, W	1470	90	0, 95, 195, 270	rock	no snow
GUN	SW, NW	1470	90	245, 330	rock	no snow
GUN	fl	1470	0	-	thin soil on rock	wind exposed
HUD	wx	1670	10	10, 220		no ground T
HUD	S2, S3, NW, N, NE	1970 (S) / 2140	50 - 90	180, 240, 285, 350, 60	rock	no snow
HUD	fl, cx	2020	0 - 10	- , 40	rock	different snow
HUD	scr1-5	2030-2160	0 - 30	190, 190, - , - , 0	coarse debris	snow covered
MID	wx	1000	0	-	soil, grass	cold air drainage
MID	pf	1010	0	-	soil & moss	palsa, black spr.
MID	fr	1020	10	210	soil & moss	spruce forest
NON	wx	1680	0	-	alpine tundra	wind exposed
NON	N, S	1670	15 - 20	0, 180	alpine tundra	wind exposed
PIN	wx	1750	0	-		no ground T
PIN	W, SE	1740	90	285, 135	rock	no snow
PIN	cx, cc	1750	0	-	alpine tundra	different snow
PIN	ls	1740	25	80	coarse debris	snow covered
POP	N1 – N3	780 - 940	15 - 30	0, 0, 10	soil & moss	black spruce f.
POP	N4*, S	940, 750	30, 15	10, 180	soil, light forest	* on landslide
POP	SW	890	35	240	fine grain. debris	colluvium
TET	S1, S2	1010	25	170	soil & moss	aspen-pine f.
TET	N1, N2	1010	25	10	soil & moss	black spruce f.

[1] location labeles: wx = weather station, cr = crack, N, E, S, W etc. = aspect, fl = flat, cx = convex, cc = concave, scr = scree, pf = permafrost, fr = forest, ls = landslide

739

740 Table 2: Surface offsets for all monitored near-vertical cliffs

site-location	*aspect* (°)	*surface offset (°C)*
GUN-N	0	0.9
GUN-E	95	2.5
GUN-S	195	5
GUN-SW	245	4
GUN-W	270	2.2
GUN-NW	330	1.1
HUD-S2	180	4.8
HUD-NW	285	1
HUD-N	350	1
PIN-SE	135	4.1
PIN-W	285	1.4

741
742

Figures

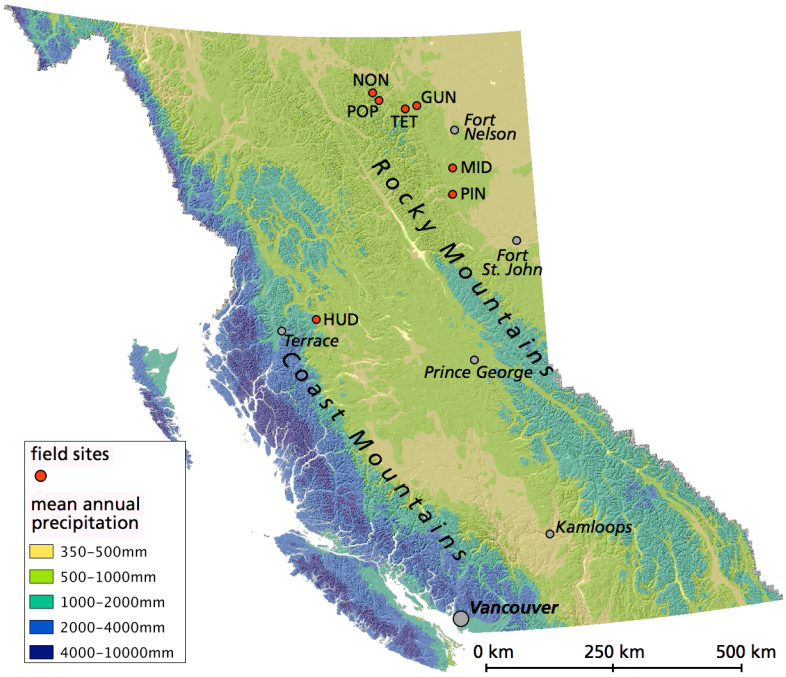

Figure 1: Overview of the field sites on a precipitation map of British Columbia. The field sites span a latitudenal range from 54°45' to 59°N and are located within or close to the Coast Mountains and Rocky Mountains. These two main mountain ranges cause large gradients in precipitation and continentality within short distance (precipitation data from Wang et al. 2012).

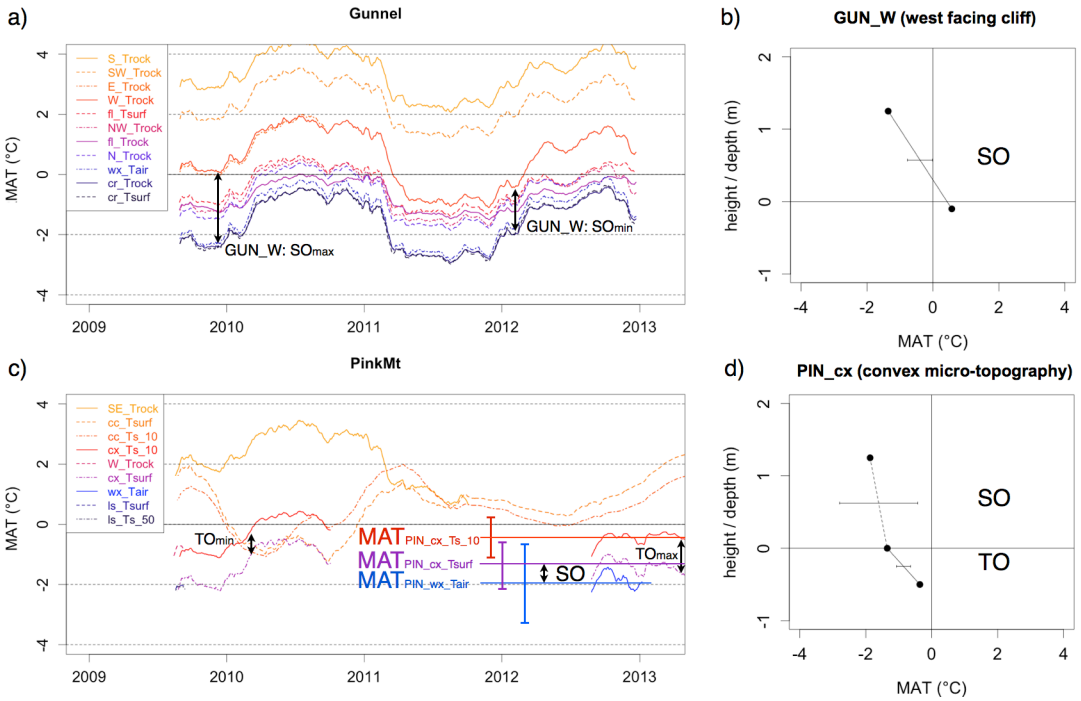

Figure 2: The running mean annual temperatures (running MAT) at two field sites and two profile plots of the MAT. a): Mt. Gunnel. All near-surface MAT from vertical rock faces have a development parallel to the mean annual air temperature (MAAT). Indications of maximum and minimum surface offset are explained in text. b) example of the surface offset (SO) shown in the MAT profile of a west facing cliff at Mt. Gunnel. The temperature at 1.4 m height is the MAAT. c): Pink Mountain. The MAT from convex (cx) and concave (cc) landforms show inverse development. Offsets strongly depend on the point in time of the comparison of instantaneous MATs. This example is a worst case in terms of data completeness. d): MAT profile with spreads indicating the uncertainties of the surface- and thermal offsets at Pink Mt. The solid lines indicates an offset that is larger than the spread (TO), the dashed line is used if offset is equal or smaller than the spread (SO).

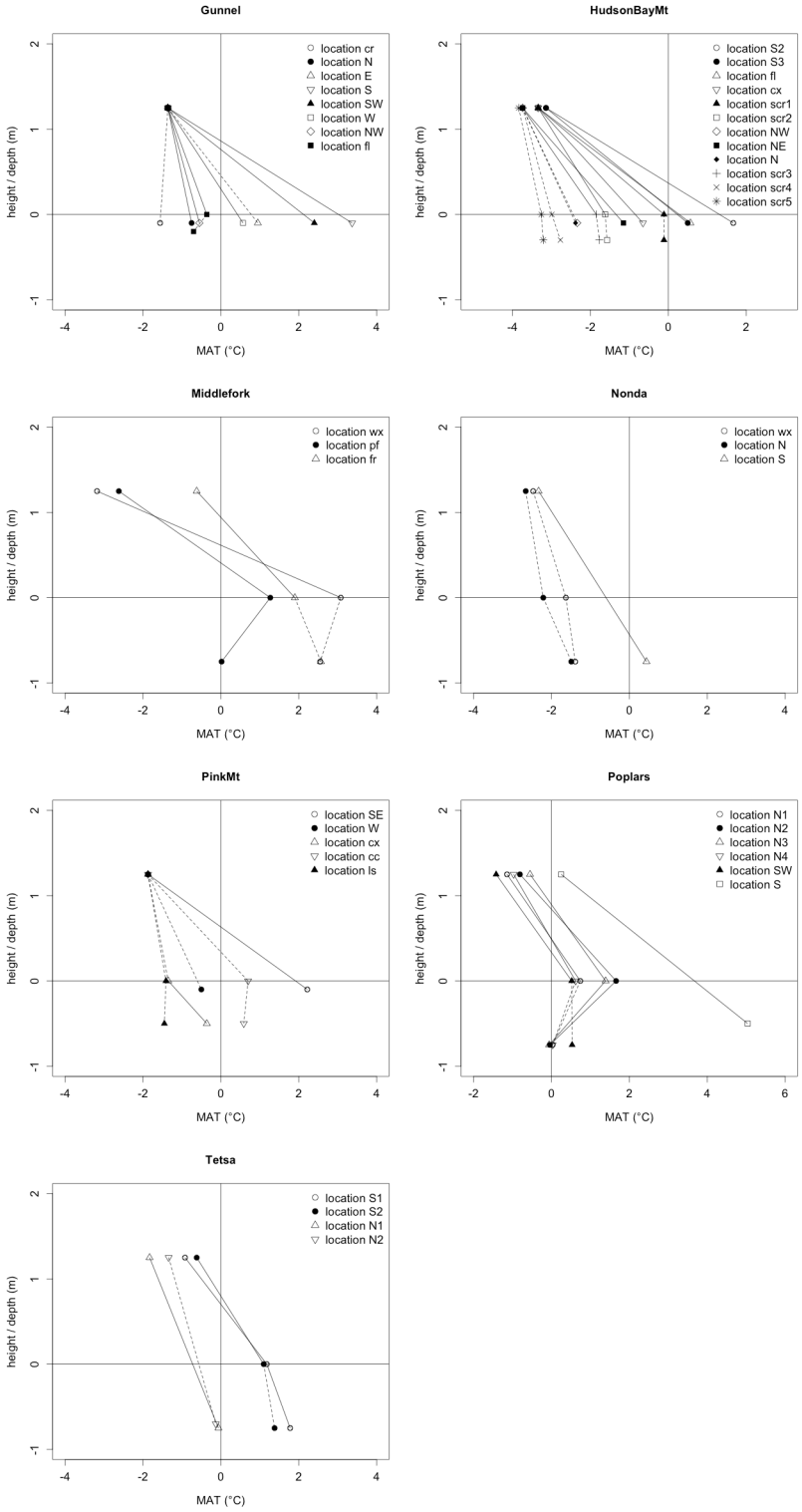

Figure 3: Overview of all thermal profiles measured at 44 locations within the seven field sites. The temperatures at 1.4 m height are the mean annual air temperatures (MAAT). Dashed lines indicate offsets below the inward uncertainty (Offset < U_{offset} / 2) of these offsets (section 3.2). Solid lines indicate significant offsets.

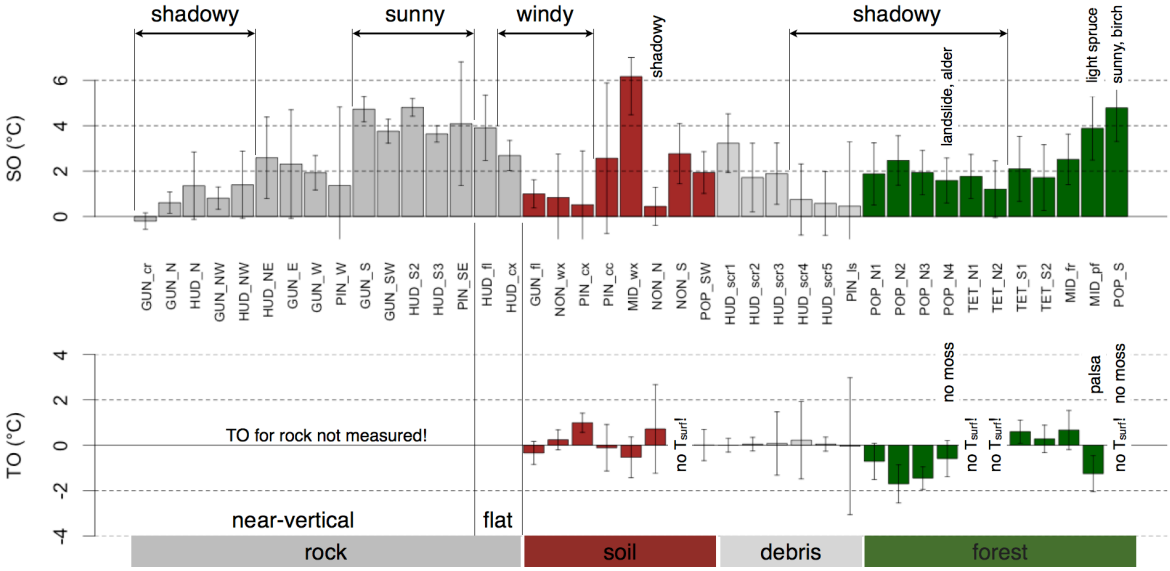

Figure 4: Surface and thermal offsets grouped by different surface types (substrate and vegetation) and with indication of micro-topographic situation and forest type.

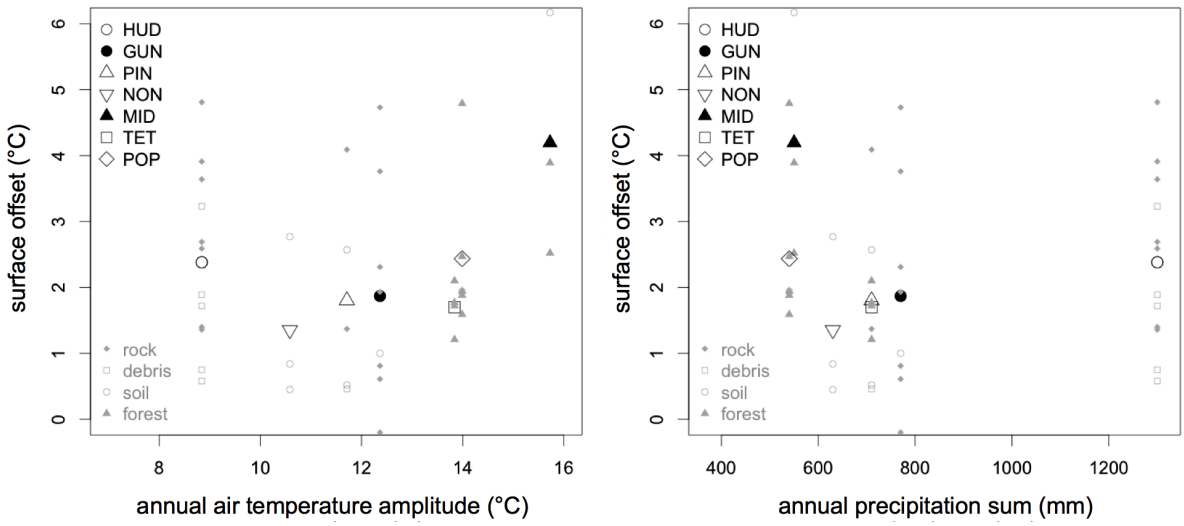

774

775 Figure 5: Surface offsets (SO) against macro-climatic parameters. Large symbols are means per site and small
776 symbols are individual locations with symbol given by surface type. Left: SO against measured annual
777 amplitude of air temperature (ATA = $(T_{july} - T_{jan})/2$); right: SO against annual precipitation sum (precipitation
778 estimate from Wang et al. 2012).

779

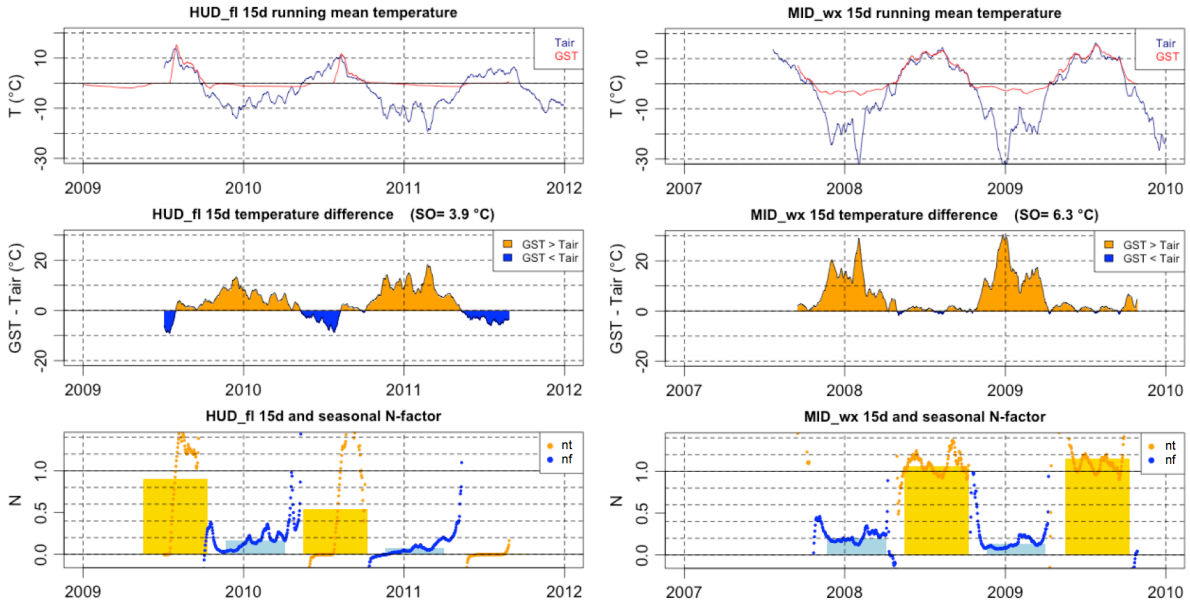

780

781 Figure 6: Seasonal development of temperature differences and N-factors at flat rock on Hudson Bay Mt. (left)
782 and in a flat meadow at Middlefork (right). Top: air and ground surface temperature (15-days running mean);
783 middle: temperature difference (GST–T_{air}) on 15-days running average; bottom: N-factors on seasonal average
784 (bars) and 15-days average (points). The SO is to one part controlled by the winter air temperature and is
785 larger at MID_wx (orange area; middle). Negative differences in early summer (blue area; middle left)
786 contribute to a smaller SO at HUD_fl. Freezing N-factors (*nf*) are on a similar level (0.1–0.2), whereas
787 thawing N-factors (*nt*) differ due to the persistence of the snow during summer at HUD_fl.

788

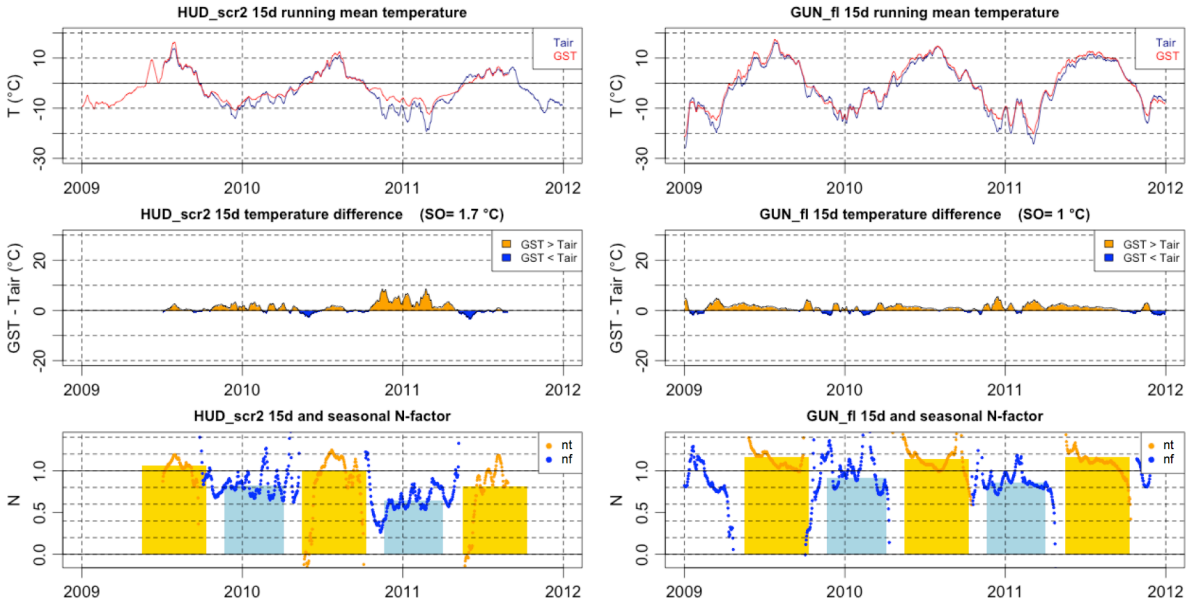

Figure 7: Seasonal development of temperature differences and N-factors in a windy scree slope at Hudson Bay Mt. (left) and on a windy plateau at Mt. Gunnel (right). Top: air and ground surface temperature (15-days running mean); middle: temperature difference (GST–T_{air}) on 15-days running average; bottom: N-factors on seasonal average (bars) and 15-days average (points). Note that the 2009 and 2011 seasonal thawing N-factors (*nt*) at *HUD_scr2* are slightly biased by the incomplete data. At both sites GST follows the air temperature. The snow cover is slightly more developed at *HUD_scr2* and reduces both, freezing and thawing N-factor.

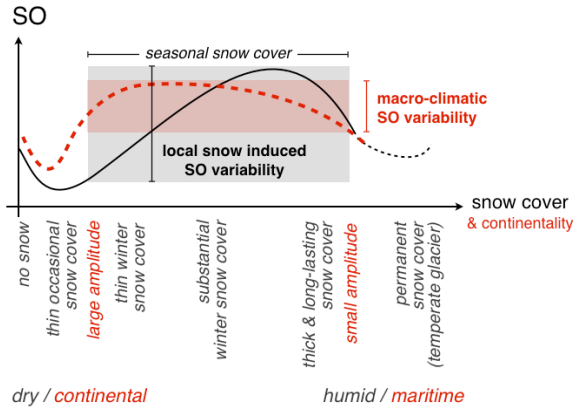

Figure 8: Qualitative sketch of the effect of snow cover and continentality on the surface offset (SO): The dashed red line indicates the dependency on a macro-climatic continentality gradient (annual air temperature amplitude) correlated with an increase in precipitation (and snow thickness; strong seasonality of precipitation is neglected). The black line corresponds to the effect of local variations in snow accumulation (wind drift etc.) but constant annual air temperature amplitude. While SO increases with snow cover thickness for local variations until the effect of snow persistence reverses the trend, the continentality effect leads to a small variation of the SO for conditions with a seasonal snow cover.